

# IMPROVING ELECTROMAGNETIC BIAS ESTIMATES

Floyd W. Millet and Karl F. Warnick

Brigham Young University, MERS Laboratory: 459 CB, Provo, UT 84602  
801-422-4884, milletf@ee.byu.edu

## Abstract

The derivation of an electromagnetic (EM) bias model that includes the physical optics scattering models and the non-Gaussian long wave surface statistics is presented. The final formulation of the model is expressed as a function of hydrodynamic modulation, surface skewness, and tilt modulation. Through the modulation transfer function, the hydrodynamic modulation coefficient is shown to be equivalent to the long wave RMS slope multiplied by a function of the short wave spectrum. With this result the normalized EM bias reduces to a function of long wave surface parameters with coefficients determined by properties of the short ocean waves. EM bias values are computed from the theory, using a realistic surface PSD, and compared with *in situ* bias measurements. The bias model is shown to be in excellent agreement with the measured values, and includes features of normalized bias not present in previous models.

## 1 INTRODUCTION

Altimeter measurements of the mean sea level are complicated by errors introduced by atmospheric propagation, satellite ephemeris, and the interaction between the electromagnetic signal and the ocean surface. As satellite technology has matured and our understanding of geophysical processes improves, errors in mean sea level measurements have been reduced to the centimeter level. The remaining uncertainty is dominated by errors in electromagnetic (EM) bias estimates.

The electromagnetic bias is caused by an unequal distribution of returned power from the crests and troughs of ocean surfaces. Larger power returns from ocean troughs than from the crests causes a time delay in the median backscattered power. Remote sensing instruments, such as altimeters, interpret this time delay as an increased distance to the surface, and causing mean sea level estimates to be lower than the true surface.

EM bias models for satellite based altimeters are limited to parameters that can be estimated from the EM backscatter characteristics of the surface.<sup>1-5</sup> Among these models are the current operational models for the TOPEX/Poseidon and Jason-1 altimeter missions that estimate the bias from significant wave height and wind

speed values. Though bias estimates using these parameters are accurate in the mean a significant amount of variance remains.<sup>6</sup>

Theoretical studies of the EM bias have shown that the bias is a composite of two underlying physical mechanisms. The non-Gaussian long wave surface statistics were used to develop the first EM bias model. Using the weakly non-linear (WNL) theory by Longuet-Higgins,<sup>7</sup> the EM bias for a one dimensional surface was described by Jackson<sup>8</sup> as a function of the skewness and tilt modulation ocean surface. The contributions of the non-Gaussian surface was expanded to two-dimensions in a work by Srokosz, et al.,<sup>9</sup> and further developed by Elfouhaily, et al.<sup>10</sup>

The second physical mechanism that contributes to the EM bias is hydrodynamic modulation. Using the theory by Longuet-Higgins<sup>11</sup> that equates the modulation coefficient with the RMS wave slope, the empirical relationship between RMS wave slope and bias been developed in a number of models.<sup>12-14</sup> This approach has been expanded recently by a pair of theoretical models. The first, by Elfouhaily, et al.,<sup>15</sup> develops a bias theory that describes the hydrodynamic modulation using the modulation transfer function (MTF) by Alpers and Hasselmann.<sup>16</sup> The second model, by Warnick, et al.,<sup>17</sup> introduces hydrodynamic modulation through the physical optics (PO) scattering model. This method results in a bias model that reflects the relationship between the bias and the RMS wave slope seen in *in situ* and laboratory measurements.

The only study to combine the non-Gaussian surface statistics with hydrodynamic modulation was a numerical study by Rodriguez, et al.<sup>18</sup> In this study, the joint height-slope PDF by Longuet-Higgins<sup>7</sup> was combined with the modulation transfer function (MTF) of Alpers and Hasselmann.<sup>16</sup> The result is a model that shows that contributions from the non-Gaussian surface statistics and hydrodynamic modulation are roughly the same.

This paper presents an EM bias model that includes both hydrodynamic modulation and non-Gaussian long wave statistics as sources of the EM bias. The non-Gaussian statistics come from the same WNL theory developed by Longuet-Higgins<sup>7</sup> and used in previous bias models. The hydrodynamic modulation is included through the use of the PO scattering model as developed by Warnick, et al.<sup>17</sup> The resulting model describes the EM bias as a sum of terms that include skewness,

peakedness, and RMS wave slope with the well-known linear dependence on significant wave height.

A number of features of the model are worth noting. First, an analytical relationship between the hydrodynamic modulation and the EM bias is shown through the use of the MTF. Second, through the PO model small wave roughness and wind speed dependence are included in the EM bias model. Finally, the results from the model show excellent agreement with measured data, including a number of data features that are not seen in previous models.

## 2 EM BIAS MODEL DERIVATION

The model derivation begins with the definition of the EM bias,  $\epsilon$ , as the normalized correlation between the surface height,  $\zeta$ , and the radar cross section at that height, or backscatter coefficient profile,  $\sigma^\circ(\zeta)$ ,

$$\epsilon = \frac{\mathbb{E}[\zeta\sigma^\circ(\zeta)]}{\mathbb{E}[\sigma^\circ(\zeta)]} = \frac{\int \int \zeta\sigma^\circ(\zeta, \theta)P(\zeta, \theta)d\zeta d\theta}{\int \int \sigma^\circ(\zeta, \theta)P(\zeta, \theta)d\zeta d\theta}. \quad (1)$$

The bias in this form is composed of the backscattered power from patches of small-scale ocean waves,  $\sigma^\circ(\zeta, \theta)$  at heights and local incidence angles described by the joint height-slope probability distribution of the surface,  $P(\zeta, \theta)$ .

The terminology that defines the bias seen by remote sensing instruments is typically divided into three contributing components: skewness bias, EM bias, and tracker bias. The tracker bias is an instrumental error that is neglected in this discussion. The skewness bias and electromagnetic bias are errors that are inherent in the signal returned from the ocean surface. These errors are often combined into a single error referred to as the sea state bias.

This derivation results in three factors that contribute to the bias seen by the instrument: skewness bias, tilt modulation bias, and hydrodynamic modulation bias. The total of these factors is referred to as the EM bias in this paper.

A number of steps are taken in the derivation of the EM bias model. First, a description of the surface is developed with long and short wave components. Next, hydrodynamic modulation is developed with the MTF. Using an analytic expression for the backscatter coefficient profile and the physical optics scattering model, and the EM bias model is developed. The last two sections review the contributions of the long and short wave components to the bias, the terms that describe the bias, and a comparison of the model to measured bias values.

### 2.1 Surface Modeling

A requirement in the derivation of EM bias models is a statistical description of the ocean spectrum. In this

paper the unified ocean spectrum by Elfouhaily, et al.<sup>19</sup> has been used as a model for a realistic ocean spectrum. The spectrum has as inputs the wind speed,  $U$  and inverse wave age,  $\Omega$ .

Division of the ocean spectrum is necessary for application of the MTF and facilitates the computation of the rough surface scattering. We identify the division between the long and short wave components of the ocean spectrum using the separation wavelength,  $\lambda_{sep} = 2\pi/k_{sep}$  such that

$$[\lambda_o = \mathcal{O}(10m)] \ll \lambda_{sep} \ll [\lambda_{em} = \mathcal{O}(10^{-2}m)] \quad (2)$$

where  $\lambda_{em}$  is the electromagnetic wavelength and  $\lambda_o$  is the dominant wavelength of the surface spectrum. We note that  $k_{sep}$  influences the small and long wave portions of the spectrum, and investigate its effect in the results section.

#### 2.1.1 Long Wave Surface Statistics

The joint height-slope distribution of the long wave surface spectrum is developed by Longuet-Higgins<sup>7</sup> in his weakly non-linear theory. The distribution used is a Gram-Charlier expansion that describes the surface as Gaussian, to first order, with modifications described by the skewness,  $\lambda_{30}$ , and peakedness or tilt modulation,  $\lambda_{12}$ , of the surface.<sup>9,10</sup> We model the long waves using the long crested assumption so that the slope in one direction is set equal to zero,  $\zeta_y = 0$ . With this approximation the three dimensional joint-height slope PDF is reduced to a two dimensional expression,

$$P(\eta, \eta_x) = \frac{e^{-\frac{1}{2}(\eta^2 + \eta_x^2)}}{2\pi h_l s_l} \times \left[ 1 + \frac{\lambda_{30}}{6} \mathcal{H}_{30}(\eta, \eta_x) + \frac{\lambda_{12}}{2} \mathcal{H}_{12}(\eta, \eta_x) \right], \quad (3)$$

where we define the normalized height and normalized slope as

$$\eta = \zeta/h_l \quad (4)$$

$$\eta_x = \zeta_x/s_l \quad (5)$$

and the height and slope variances are described by  $h_l^2$  and  $s_l^2$  respectively. The Hermite polynomials,  $\mathcal{H}_{ij}(\eta, \eta_x)$ , used in this paper are

$$\mathcal{H}_{30} = \eta^3 - \eta \quad (6)$$

$$\mathcal{H}_{12} = \eta(\eta_x^2 - 1) \quad (7)$$

where we drop the explicit dependencies on height and slope.<sup>9</sup>

#### 2.1.2 Short Wave Surface Spectrum

With the definition of the separation wave number above, the short wave surface spectrum is defined by

$$W_s(\mathbf{k}) = W(\mathbf{k}), \quad k > k_{sep} \quad (8)$$

where  $W(\mathbf{k})$  is the full surface spectrum, with the related correlation function is defined as

$$C(x, y) = \frac{1}{h^2} \int W_s(\mathbf{k}) e^{i\mathbf{k}\cdot\mathbf{r}} d\mathbf{k}. \quad (9)$$

where  $C(x, y)$  is the Fourier transform of the short wave PSD normalized by the surface height variance,  $h^{-2}W(\mathbf{k})$ .

It should be noted that the small waves are described by a two-dimensional isotropic spectrum. This leads to the development of an EM bias model using scattering from two-dimensional small wave facets of the surface on a corrugated, or one-dimensional, long wave surface.

## 2.2 Hydrodynamic Modulation

The modulation of short wave heights as a function of surface displacement causes a differential in surface roughness between the crests and troughs of the ocean surface. This results in a larger specular return from the troughs, contributing to the energy differential that is the cause of the EM bias. We refer to this contribution to the EM bias as the hydrodynamic bias.

Short wave height modulation is described by a modulation transfer equation (MTF). The MTF, developed by Alpers and Hasslemann<sup>16</sup> and used by Rodriguez, et al.<sup>18</sup> and Elfouhaily, et al.<sup>15</sup> in previous EM bias studies, describes the height modulation of short waves over the phase of longer ocean waves as a function of spectral frequency,

$$\delta W(k_s) = W(k_s) \int dk_l z(k_l) R(k_s, k_l) e^{i(k_l x - \omega_l t)} \quad (10)$$

where  $z(k_l)$  is the Fourier transform of the long wave profile,  $\zeta(x, t)$ , and  $\omega_l$  and  $k_l$  are the long wave angular frequency and wavenumber, respectively. The one dimensional form of the modulation transfer function can be written as

$$R(k_s, k_l) = k_l \frac{\omega_l + i\mu_s}{\omega_l^2 + \mu_s^2} \frac{c_l}{c_s} \left[ \frac{1}{F(k)} \frac{\partial F(k)}{\partial k} - \frac{\gamma_s}{k_s} \right] \times \left( c_s k_l k_s - \frac{1}{2} k_l \omega_l \right) \quad (11)$$

where  $\mu_s$  is the short wave relaxation rate,  $c_l$  and  $c_s$  are the long wave and short wave phase speeds,

$$\gamma_s = \frac{1}{2} \frac{1 + 3(\tau k_s^2 / \rho g)}{1 + \tau k_s^2 / \rho g} \quad (12)$$

and the constants  $\tau = 74 \times 10^{-6} \text{ m}^3/\text{s}^2$  and  $\rho = 1027 \text{ kg}/\text{m}^3$  are the surface tension and water density.

## 2.3 Physical Optics Scattering Model

The rough surface scattering model has an important influence in developing a model for the EM bias. The most

common scattering model used in EM bias theories is the geometrical optics (GO) model. Geometrical optics uses the infinite frequency, or ray tracing, approximation to model scattering from a rough surface. With this approximation surfaces are considered smooth with respect to the incident EM wavenumber, thus applying an inherent high wavenumber cutoff to the surface spectrum. The use of GO in EM bias models is complicated by hydrodynamic modulation. Because the modulated wave small wave heights are on the same order of magnitude as the incident wavenumber, the GO approximation does not apply.

A more accurate description of rough surface scattering is provided by the physical optics (PO) scattering model,

$$\sigma^\circ(\theta) = \frac{k_{em}^2 \cos^2 \theta}{4\pi} \int \int e^{ik_b x} e^{-\lambda(1-C(x,y))} dx dy, \quad (13)$$

where the Bragg wavenumber,  $k_b = 2k_{em} \sin \theta$ , and  $\lambda = (2k_{em} h \cos \theta)^2$ . The PO model includes the surface height variance,  $h^2$ , and the correlation function,  $C(x, y)$ , as input parameters, and has been shown to accurately model scattering from ocean-like surfaces.<sup>20,21</sup>

The first EM bias model to use the physical optics (PO) scattering model was developed in Warnick, et al.<sup>17</sup> By parameterizing the short wave height as a function of surface elevation, hydrodynamic modulation entered the EM bias model through  $h(\zeta)$ . The result was a description of the bias as a function of RMS wave slope that was strongly correlated to measured EM bias values.

This model is developed in the same form as that seen in Warnick, et al.,<sup>17</sup> with the addition local tilt angles for the small wave facets. We have already discussed the elevation and tilting of the scattering facets in the description of the long wave joint height-slope PDF. In this section we describe the correlation function,  $C(x, y)$ , and the short wave surface height,  $h$ , used in this model.

### 2.3.1 Correlation Function

The correlation function required by the PO scattering model can, in theory, be computed directly as the Fourier transform of the short wave power spectrum,  $W_s(k)$ , in equation 8. However, direct calculation of the two-dimensional Fourier transform is computational prohibitive. Instead, we model the small wave power spectrum as a power law fit to the two dimensional, omnidirectional, unified spectrum described by Elfouhaily, et al.<sup>19</sup> The short wave portion of the unified surface spectrum can be modeled as

$$W(k) = \begin{cases} h^2(p-2)k_{sep}^{p-2}k^{1-p} & k \geq k_{sep} \\ 0 & k < k_{sep} \end{cases} \quad (14)$$

where  $W(k)$  is the surface PSD and the values of  $h^2$  and  $p$  are calculated from fits to the unified surface spec-

trum. The correlation function associated with a power law power spectrum for  $p \neq 3$  is defined by

$$C(x) = (p-2)x^{p-2}2^{1-p}\frac{\Gamma(1-\frac{p}{2})}{\Gamma(\frac{p}{2})} + \mathcal{HY}\mathcal{P}\left(\left[1-\frac{p}{2}\right], \left[1, 2-\frac{p}{2}\right], -\frac{x^2}{4}\right) \quad (15)$$

where  $\mathcal{HY}\mathcal{P}$  is the hypergeometric function. A similar expression can be developed for  $p = 3$ , that is similar to equation (15) In the remainder of the paper, the explicit dependence on distance of the correlation function is dropped so that  $C = C(x, y)$ .

### 2.3.2 Hydrodynamic Modulation

The change in small wave surface height with surface displacement defines the hydrodynamic modulation. For a surface with no modulation, the standard deviation of the small waves is described by a constant,  $h = h_o$ . To include the hydrodynamic modulation, we parameterize the short wave height variance with surface height,  $h(\zeta)$ . Figure 1 shows the modulation in the short wave variance as a function of surface height when the MTF is applied to surface described by the unified surface spectrum. A numerical study by Rodriguez, et al.<sup>18</sup> and experimental measurements of small wave surface heights showed a similar relationship.<sup>17</sup> From these studies the short wave height standard deviation can be described by

$$h(\zeta) = h_o \left(1 + m \frac{\zeta}{h_l}\right) \quad (16)$$

where  $h_o$  is the average short wave standard deviation and  $m$  is the modulation coefficient.

## 2.4 Backscatter Coefficient Profile

An analytic expression for the backscatter coefficient profile,  $\sigma^\circ(\zeta)$ , is created from expressions for the long wave joint height-slope PDF, (4), and the small wave scattering described by the PO model, (13). Using the approximations for the correlation function, (15), and hydrodynamic modulation, (16), the resultant expression

$$\begin{aligned} \sigma^\circ(\zeta) &= \frac{k_{em}^2 \cos^2 \theta}{4\pi} \int d \tan \theta \\ &\times \int \int dx dy e^{i2k_{em} \sin \theta} e^{-\lambda(\eta)(1-C)} \\ &\times \frac{1}{2\pi h_l s_l} e^{-\frac{1}{2} \left[ \left(\frac{\zeta}{h_l}\right)^2 - \left(\frac{\tan \theta}{s_l}\right)^2 \right]} \\ &\times \left(1 + \frac{\lambda_{30}}{6} \mathcal{H}_{30} + \frac{\lambda_{12}}{2} \mathcal{H}_{12}\right) \end{aligned} \quad (17)$$

is a three-dimensional integral that appears in both the numerator and denominator of the EM bias definition,

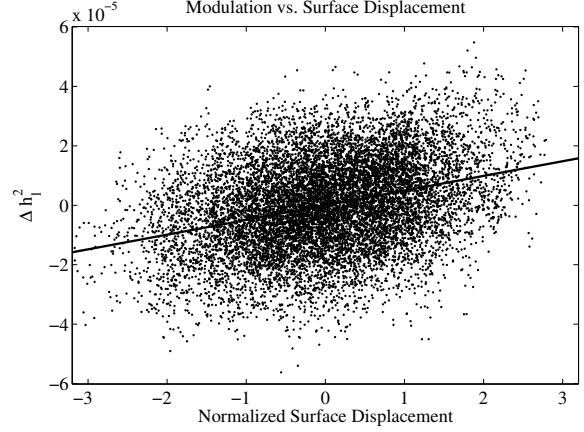


**Figure 1:** Application of the modulation transfer function (MTF) to surface described by the unified ocean spectrum by Elfouhaily, et al.<sup>19</sup> shows a linear correlation between the magnitude of the short wave modulation and the normalized surface height.

(1). Because the leading coefficient,  $(k_{em} \cos \theta)^2/4\pi$ , appears in both numerator and denominator in the bias definition, it will ultimately cancel out, and is dropped in the remainder of the derivation.

To simplify the computation of  $\sigma^\circ(\zeta)$ , the assumption of small local incidence angles is made such that

$$\sin \theta \approx \theta \quad (18)$$

$$\cos \theta \approx 1 \quad (19)$$

$$\tan \theta \approx \theta. \quad (20)$$

The order of integration is also changed so that the first integral performed is the integral over the long wave slopes,

$$\begin{aligned} \sigma^\circ(\zeta) &= \frac{e^{-\eta^2/2}}{\sqrt{2\pi}} \int \int dx dy e^{-\lambda(\eta)(1-C)} \\ &\times \int d\eta_x e^{i\mu\eta_x} \frac{e^{-\eta_x^2/2}}{\sqrt{2\pi}} \\ &\times \left(1 + \frac{\lambda_{30}}{6} \mathcal{H}_{30} + \frac{\lambda_{12}}{2} \mathcal{H}_{12}\right) \end{aligned} \quad (21)$$

where  $\mu = 2xk_{em}s_l$ . The expression inside the last integral can be seen as a Fourier transform that with the identities

$$\int e^{i\mu x} x^2 e^{-x^2/2} dx = \sqrt{\frac{\pi}{2}} e^{-\mu^2/2} (1 - \mu^2) \quad (22)$$

$$\int e^{i\mu x} e^{-x^2/2} dx = \sqrt{2\pi} e^{-\mu^2/2}. \quad (23)$$

can be solved analytically. A simplified expression for equation (21) can be written

$$\begin{aligned} \sigma^\circ(\zeta) &= \frac{e^{-\eta^2/2}}{\sqrt{2\pi}h_l} \int dx dy e^{-\lambda(\eta)(1-C)} e^{-\mu^2/2} \quad (24) \\ &\times \left( 1 + \frac{\lambda_{30}}{6} (\eta^3 - \eta) - \frac{\lambda_{12}}{4} \eta (1 - \mu^2) \right), \end{aligned}$$

and the expression for the backscatter coefficient profile is reduced to a two dimensional integral in the  $x$  and  $y$  dimensions.

## 2.5 EM Bias

The final expression of the EM bias model is created by expanding the definition of the EM bias in equation (1) in a power series about  $\zeta = 0$ ,

$$\epsilon = \frac{E[\zeta(\sigma^\circ(0) + \zeta\sigma^{\circ\prime}(0) + \dots)]}{E[\sigma^\circ(0) + \zeta\sigma^{\circ\prime}(0) + \dots]}. \quad (25)$$

where  $\zeta\sigma^{\circ\prime}(0)$  refers to the derivative of  $\sigma^\circ(\zeta)$  with respect to  $\zeta$ . Results from the model by Warnick, et al.<sup>17</sup> show that the average backscatter coefficient is linear with displacement, and the expression in equation (25) can be truncated after the linear term.

Using this approximation, equation (25) reduces to

$$\epsilon \approx h_l \frac{\sigma^{\circ\prime}(0)}{\sigma^\circ(0)}. \quad (26)$$

where to compute the bias only the numerator

$$\begin{aligned} \sigma^{\circ\prime}(0) &= \frac{-1}{\sqrt{2\pi}} \int \int dx dy e^{-(2kh_o)^2(1-C) - \mu^2/2} \times \\ &\left[ 8m(kh_o)^2(1-C) + \frac{\lambda_{30}}{6} + \frac{\mu^2\lambda_{12}}{2} \right] \quad (27) \end{aligned}$$

and denominator

$$\sigma^\circ(0) = \frac{1}{\sqrt{2\pi}} \int \int dx dy e^{-(2kh_o)^2(1-C) - \mu^2/2} \quad (28)$$

are needed. The notation can be simplified by writing the expression for the EM bias as

$$\epsilon = -H(\gamma m + \kappa\lambda_{30} + \tau\lambda_{12}). \quad (29)$$

where the significant wave height is  $H = 4h_l$ , and the coefficients  $\gamma$ ,  $\kappa$ , and  $\tau$  are defined by

$$\begin{aligned} \gamma &= \frac{\int \int 2k_{em}^2 h_o^2 (1-C) e^{-(2k_{em}h_o)^2(1-C)} e^{-\mu^2/2} dx dy}{\int \int e^{-(2k_{em}h_o)^2(1-C)} e^{-\mu^2/2} dx dy} \\ \tau &= \frac{1}{8} \frac{\int \int \mu^2 e^{-(2k_{em}h_o)^2(1-C)} e^{-\mu^2/2} dx dy}{\int \int e^{-(2k_{em}h_o)^2(1-C)} e^{-\mu^2/2} dx dy} \\ \kappa &= \frac{1}{24} \quad (30) \end{aligned}$$

A quick review of the final bias model in equation (29) shows the leading  $H$  dependence, common to all bias models, followed by terms relating the bias to the surface skewness, peakedness, and hydrodynamic modulation. An in-depth analysis of the terms and coefficients that describe the model are conducted in the following sections.

## 3 EVALUATING THE BIAS

The contributions of each term in the bias model can be more fully understood by individual analysis. We begin by dividing the contribution from the modulation coefficient,  $m$ , into a function of the long wave RMS slope,  $S$ , and a short wave function,  $g$ . Following this division the contributions of the long wave components,  $\lambda_{30}$  and  $\lambda_{12}$ , and short wave components,  $\gamma$ ,  $\tau$ , and  $\kappa$ , are investigated. A comparison of the contribution of each term when compared with previous models is included.

### 3.1 Modulation Coefficient and Wave Slope

A number of EM bias models have derived an empirical relationship between the RMS long wave slope and the modulation coefficient.<sup>12,14</sup> The first model to explicitly derive a relationship between the small wave modulation and RMS slope was Melville, et al.<sup>13</sup> In the model, the two frequency surface model by Longuet-Higgins<sup>11</sup> showing that to first order the modulation coefficient and RMS wave slope are equal was used. Warnick, et al.<sup>17</sup> used the same relationship and found that the RMS wave slope was strongly correlated, but that theoretical values consistently overestimated the bias.

The relationship between the short wave modulation and the RMS wave slope can be generalized as

$$m = g(p, U)S, \quad (31)$$

where  $U$  is the wind speed and  $p$  is the short wave spectral exponent. The behavior of the modulation coefficient as a function of  $p$  and  $U$  for a constant wave slope can be modeled using an idealized power law PSD,  $k^{-p}$ . Figure 2 shows the ratio of  $m/S$  for short wave PSDs with the exponents of  $p = 3, 3.5, \text{ and } 4$  at different wind speeds, where the value of  $g(p, U)$  decreases with increasing wind speed and decreasing values of  $p$ .

### 3.2 Skewness and Tilt Modulation

The skewness bias and tilt modulation bias are a direct result of the WNL theory by Longuet-Higgins,<sup>7</sup> and can be described as integral functions of the long wave portion of the surface PSD. The definitions and equations describing these values are included here for completeness and convenience.

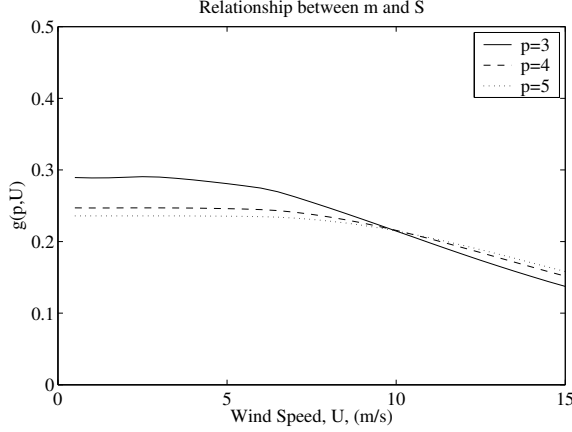


**Figure 2:** The relationship between the modulation coefficient,  $m$ , and the RMS wave slope,  $S$ , is modified by the wind speed. The effect of the wind speed is realized through the modulation transfer function. The ratio of  $m/S$  is shown for a  $k^{-p}$  short wave power law spectrum for values of  $p = 3, 4$ , and  $5$ .

The long wave skewness is defined by

$$\lambda_{30} = \frac{\langle \zeta^3 \rangle}{\langle \zeta \rangle^{3/2}} \quad (32)$$

and can be computed from the long wave surface components using

$$\lambda_{30} = \frac{12}{h_l^{3/2}} \int_0^{k_{sep}} dk W(k) \left[ \int_0^k dl l W(l) \right] \quad (33)$$

as described by Longuet-Higgins<sup>7</sup> and Jackson.<sup>8</sup> The behavior of  $\lambda_{30}$  as a function of wind speed is shown in figure 3.

The definition of the long wave peakedness is

$$\lambda_{12} = \frac{\langle \zeta \zeta_x^2 \rangle}{\langle \zeta \rangle^{1/2} \langle \zeta_x \rangle}. \quad (34)$$

Jackson<sup>8</sup> showed that with the WNL theory, the surface peakedness can be calculated as

$$\lambda_{12} = \frac{4}{h_l s_l^2} \int_0^{k_{sep}} dk W(k) \times \int_0^k dl (2k^2 l + l^3) W(l). \quad (35)$$

The tilt modulation as a function of wind speed is shown in figure 4.

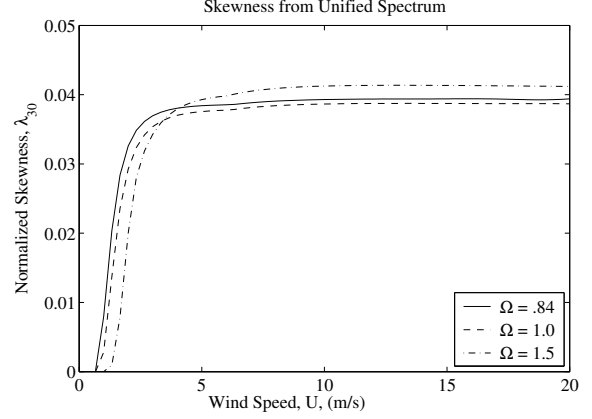


**Figure 3:** Long wave skewness values computed from the Unified Spectrum by Elfouhaily, et al.<sup>19</sup> The input parameters for this surface spectrum model are wind speed,  $U$ , and inverse wave age,  $\Omega$ .

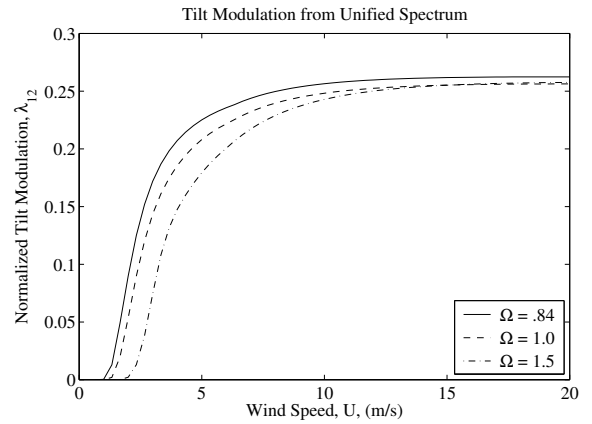


**Figure 4:** Long wave tilt modulation values computed from the Unified Spectrum by Elfouhaily, et al.<sup>19</sup> The input parameters for this surface spectrum model are wind speed,  $U$ , and inverse wave age,  $\Omega$ .

### 3.3 Bias Coefficients

The contributions of the  $\lambda_{30}$ ,  $\lambda_{12}$ , and  $m$  are modified by the coefficients,  $\gamma$ ,  $\kappa$ , and  $\tau$ . The coefficients are primarily functions of the short wave spectrum, and are present as a result of the PO scattering model. Of special interest is the relationship of  $\kappa$ , and  $\tau$ , with equivalent coefficients derived from models based on the GO scattering approximation.

#### 3.3.1 Hydrodynamic Modulation Coefficient

From the EM bias model by Warnick, et al.,<sup>17</sup> the value of  $\gamma$  was shown to asymptotically approach  $1/(p - 2)$ .

This bias model did not include the contribution of the long wave tilting of short waves. Figure 5 shows that the addition of long wave tilting has a negligible effect on asymptotic value of  $\gamma$ . We note that with typical values of  $h$  between 2-3 cm and  $k_{em} > 100$ , the value of  $\gamma$  can be considered a constant in the final EM bias model.

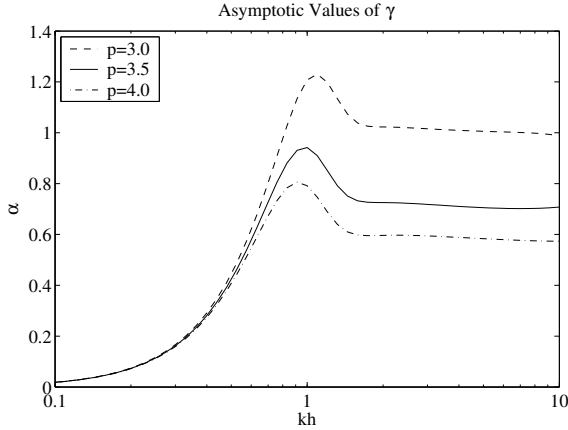


**Figure 5:** The value of  $\gamma$  determines the contribution of hydrodynamic modulation to EM bias. Values of  $\gamma$  as a function of the electromagnetic height of short ocean waves,  $kh$ , are shown for a short wave power law PSD,  $K^{-p}$  for representative exponents,  $p = 3$  and 4. The asymptotic value of  $\gamma$  approaches a constant value of approximately  $1/(p - 2)$  for all cases.

### 3.3.2 Tilt Modulation Coefficient

The inherent peakedness of the ocean causes fewer nadir pointing facets to be present near the crests of ocean surfaces, thus introducing a tilt modulation bias. For a surface smooth on the order of the incident EM wavelength, the tilt modulation results in a larger specular return from the troughs than the crests. By using the GO approximation, the model by Sorkosz, et al.<sup>9</sup> inherently uses the smooth surface approximation, resulting in a tilt modulation bias described by

$$\tau = -\frac{1}{8}\lambda_{12}. \quad (36)$$

The contribution of the tilt modulation bias is modified when surface include small scale roughness. Figure 6 shows that the value of  $\tau$  as a function of the electromagnetic height,  $k_{em}h$ , where the GO approximation is equivalent to  $kh = 0$ . With increased values of  $k_{em}$  the surface scattering is more Lambertian. The result is a decrease in the effect of the local incidence angle on backscattered power, and a decreased contribution of  $\lambda_{12}$  to the EM bias.

The change in  $k_{em}h$  can also be seen as a frequency dependent term, where the increase in  $k_{em}$  is equivalent to an increase in the small wave heights. The change in EM bias as a function of frequency is the result of changes in the tilt modulation bias with incident wavenumber.

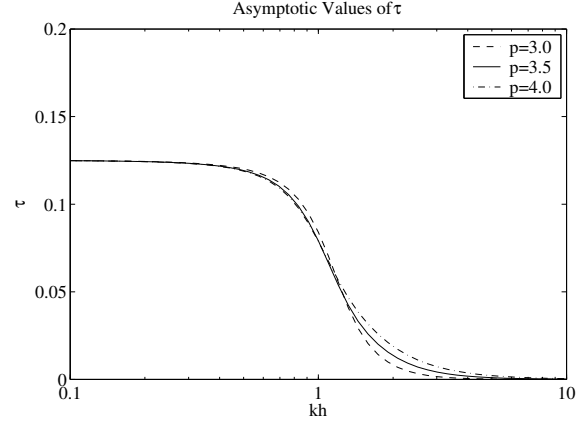


**Figure 6:** The contribution of the height-tilt variance correlation,  $\lambda_{12}$  is determined by the value of  $\tau$  shown here as a function of the electromagnetic height of short ocean waves. The asymptotic value of  $\tau$  approaches a constant value of  $1/8$ .

### 3.3.3 Skewness Coefficient

From equation (30), the skewness bias coefficient has a constant value of  $\kappa = 1/24$ . Different than  $\gamma$  and  $\tau$ , the contribution of the skewness bias is not frequency dependent. This result is identically equal to the results from the models by Srokosz and Elfouhaily, et al.

## 4 RESULTS

The accuracy of the EM bias model is analyzed by comparison to *in situ* EM bias measurements made during the Gulf of Mexico Experiment (GME).<sup>22</sup> Data from the GME consists of concurrent measurements of environmental variables and the ocean surface that allows the correlation of wind speed and significant wave height with the EM bias.

### 4.1 Separation Wavenumber

To compute the long and short wave model parameters from the unified spectrum, the separation wavelength must be set. Because the value of  $k_{sep}$  influences the long and short wave values, it can have a significant effect on estimated bias values. Figure 7 shows the change in EM bias values for various values of  $k_{sep}$ . For *in situ* measurements, the separation wavelength is constrained

to values greater than the radar spots size. With this constraint, the separation wavenumber used for this study is  $k_{sep} = 4\pi/5$ , that corresponds to a 2.5 m footprint for the GME experiment.

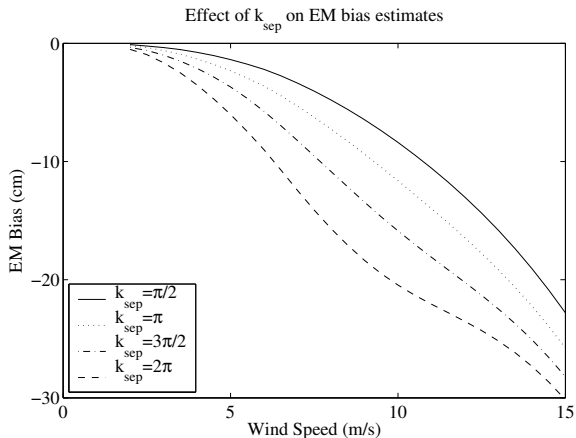


**Figure 7:** Effect of the separation wavenumber,  $k_{sep}$ , on EM bias values.

#### 4.2 Wind Speed Dependence

The behavior of the EM bias computed from the unified surface spectrum is shown in figure 8. Measured values from the GME experiment are included in the figure as a qualitative comparison. Similarities in the curvature of the bias and the zero intercept for  $U = 0$  are readily apparent. Figure 9 shows normalized bias values as a function of wind speed for a surface described by the unified spectrum. Both theoretical and measured values of the normalized bias exhibit non-zero intercepts for low wind speeds. The lack of theoretical values for low wind speeds,  $U < 2$ , is the result of the minimum wave number being greater than  $k_{sep}$ . This causes  $H = 0$  so that values that are computed with  $h_l$  in the denominator have infinite values.

#### 4.3 Model Accuracy

Application of the model to measured values of the surface is done by reviewing the surface profiles from the GME experiment and computing the tilt modulation and skewness parameters. The parameters were computed from the surface PSDs, as described in equation (36) and equation (33) as well as by direct measurements from the surface profiles. A pseudo time series plot of slope, skewness, and tilt modulation is shown in figure 10.

The small wave dependence of the EM bias is computed using constant values for the coefficients,  $\gamma$ ,  $\tau$ , and  $g$ . This approximation eliminates the inconsistencies and small wind speeds, and eliminates the need of choosing

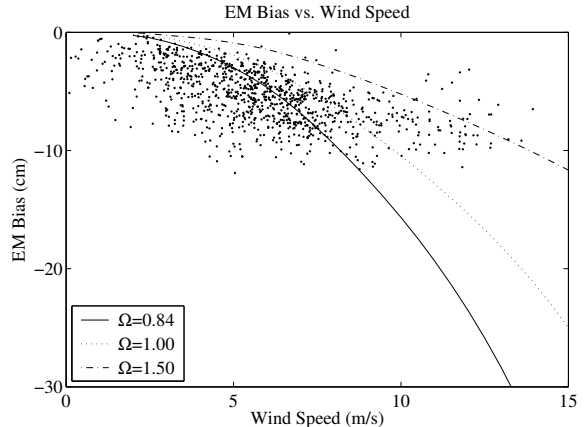


**Figure 8:** EM bias values computed from the unified surface spectrum by Elfouhaily, et al.<sup>19</sup> as a function of wind speed and inverse wave age.

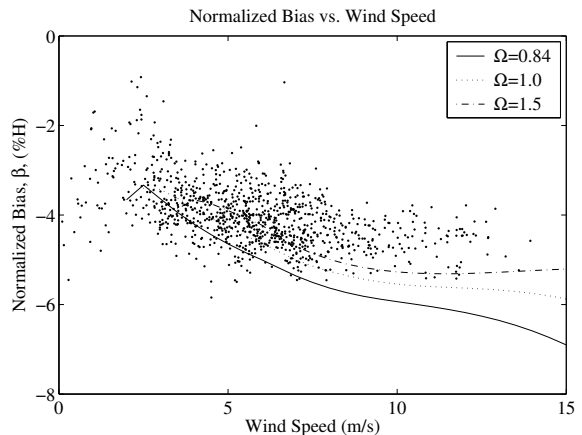


**Figure 9:** Normalized EM bias values computed from the unified surface spectrum by Elfouhaily, et al.<sup>19</sup> as a function of wind speed and inverse wave age.

the appropriate inverse wave age for the GME data set. Values of the small wave parameters are the  $\gamma = .42$ ,  $g = .63$ , and  $\tau = .11$ . Figure 11 shows pseudo-time plots of the normalized bias. The top plot shows measured bias values compared against the values from the model with the GME values for  $S$ ,  $\lambda_{12}$ , and  $\lambda_{12}$ . The bottom plot shows the contribution from each component of the EM bias: skewness bias, tilt modulation bias, and hydrodynamic modulation bias.

#### 4.4 Frequency Dependence

The frequency dependence of the model is shown in figure 12, where increases in  $k_{em}$  are accompanied by decreases in the observed bias. The frequency dependence

enters the EM bias model through the value of  $k_{em}$  in the modulation coefficient. Because the value of  $\gamma$  is close to the asymptotic limit in normal conditions, this decrease is primarily a result of the change in the value of  $\tau$ , as observed in figure (6).

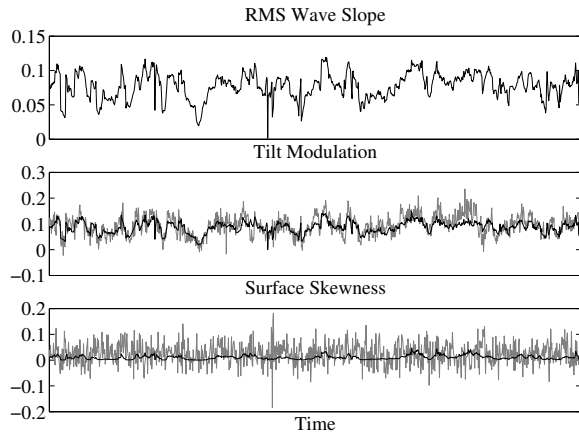


**Figure 10:** Long wave parameters computed from the GME experiment. Values for the skewness,  $\lambda_{30}$ , and the tilt modulation,  $\lambda_{12}$  are computed from the surface height PSD (black), (33) and (36) and directly from the surface profiles (gray).

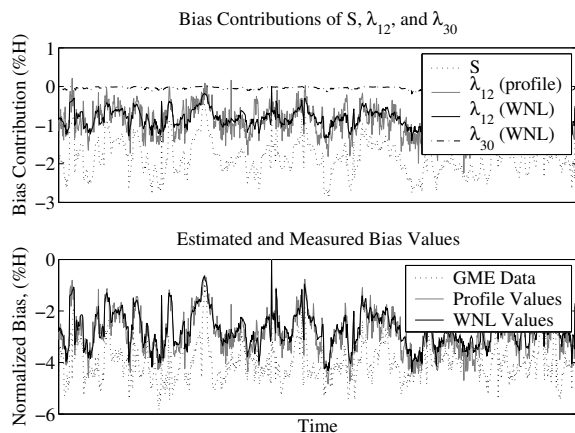


**Figure 11:** Bias values computed from GME measurements. The contribution of each long wave parameter,  $\gamma g S$ ,  $\tau \lambda_{12}$ , and  $\kappa \lambda_{30}$  is shown in the upper plot. The contribution of the tilt modulation,  $\lambda_{12}$  is shown as computed from the surface profiles and from the surface height PSD.

## 5 DISCUSSION

This paper discusses the derivation of a model based on the physical optics scattering model with the inclusion of non-Gaussian long wave surface statistics. The final form of the model includes the well-known linear dependence on the significant wave height, with further dependence described by other surface parameters. Contributions to the bias included the long wave parameters, skewness, peakedness, or tilt modulation, and RMS wave slope. The coefficients of these parameters were derived as function of the short wave surface spectrum.

By deriving a model for the EM bias using the physical optics scattering model, the hydrodynamic modulation can be included by parameterizing it as a function of surface height. This simplifies the inclusion of the hydrodynamic modulation over previous methods, and results in a simple expression relating the contribution of the hydrodynamic modulation to the EM bias.

Previous models have used equated the RMS wave slope with the modulation coefficient to derive the EM bias as a function of the RMS wave slope. Using the modulation transfer function a more formal description of the relationship between the RMS slope and the modulation coefficient is developed.

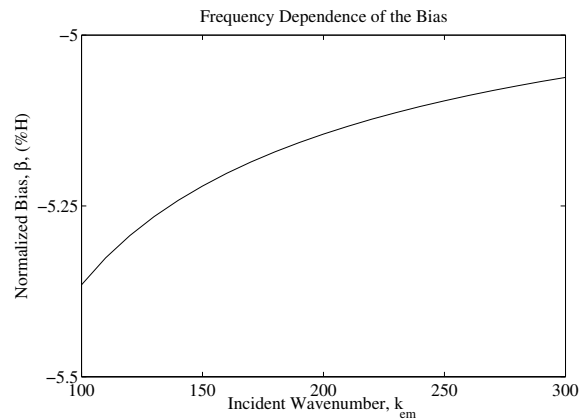


**Figure 12:** The magnitude of the EM bias decreases as a function of the incident wavenumber showing the frequency dependence of the EM bias. The frequency dependence is almost entirely due to the change in the tilt modulation coefficient with  $k_{em}$ .

Surface skewness and tilt modulation are included in the EM bias model through a Gram-Charlier expansion used by other. The contributions of these terms show similarities to previous models, but are modified by coefficients that are introduced by inclusion of the PO model. The coefficients, as functions of the small wave spectrum, modify the contributions of the long wave components with changes in small wave heights. These reasons

are explained in terms of the physics related to rough surface scattering. The cause of the frequency dependence of the EM bias model is also observed.

A qualitative comparison of numerical EM bias values computed using a realistic surface spectral model show good agreement with measured bias values. A number of features, including the roll-off in bias values with increasing wind speeds, not present in previous models were observed. Further analysis was conducted using measured long wave surface parameters to compute bias values. A strong correlation between the measured and computed EM bias values was seen. The frequency dependence of the model is also shown.

### References

- [1] Dudley B. Chelton, "The sea state bias in altimeter estimates of sea level from collinear analysis of TOPEX data," *Journal of Geophysical Research*, vol. 99, no. C12, pp. 24,995–25,008, December 15 1994.
- [2] Philippe Gaspar, Françoise Ogor, Pierre-Yves Le Traon, and Ouan-Zan Zanife, "Estimating the sea state bias of the TOPEX and POSEIDON altimeters from crossover differences," *Journal of Geophysical Research*, vol. 99, no. C12, pp. 24,981–24,994, December 15 1994.
- [3] Philippe Gaspar and Jean-Pierre Florens, "Estimation of the sea state bias in radar altimeter measurements of sea level: Results from a new nonparametric method," *Journal of Geophysical Research*, vol. 103, no. C8, pp. 15,803–15,814, July 15 1998.
- [4] P. Gaspar, S. Labroue, F. Ogor, G. Lafitte, L. Marchal, and Magali Rafanel, "Improving nonparametric estimates of the sea state bias in radar altimetry measurements of sea level," In review, 2001.
- [5] Ernesto Rodriguez and Jan M. Martin, "Estimation of the electromagnetic bias from retracked TOPEX data," *Journal of Geophysical Research*, vol. 99, no. C12, pp. 24,971–24,979, December 15 1994.
- [6] F. Millet, D. Arnold, P. Gaspar, K. Warnick, and J. Smith, "Electromagnetic bias estimation using *in situ* and satellite data: A nonparametric approach," *IEEE Journal of Geophysical Research*, vol. 108, no. C2, pp. 3041, 2003.
- [7] M. S. Longuet-Higgins, "The effect of non-linearities on statistical distributions in the theory of sea waves," *Journal of Fluid Mechanics*, vol. 17, pp. 459–480, 1963.
- [8] F. C. Jackson, "The reflection of impulses from a nonlinear random sea," *Journal of Geophysical Research*, vol. 84, pp. 4939–4943, 1979.
- [9] M. A. Srokosz, "On the joint distribution of surface elevation and slopes for a nonlinear random sea, with an application to radar altimetry," *Journal of Geophysical Research*, vol. 91, no. C1, pp. 995–1006, January 15 1986.
- [10] T. Elfouhaily, D. R. Thompson, B. Chapron, and D. Vandemark, "Improved electromagnetic bias theory," *Journal of Geophysical Research*, vol. 105, no. C1, pp. 1299–1310, January 15 2000.
- [11] M. S. Longuet-Higgins, "The propagation of short surface waves on longer gravity waves," *Journal of Fluid Mechanics*, vol. 177, pp. 293–306, 1987.
- [12] F. Millet, D. Arnold, K. Warnick, and J. Smith, "Electromagnetic bias estimation using *in situ* and satellite data: The wave slope argument," *IEEE Journal of Geophysical Research*, vol. 108, no. C2, pp. 3040, 2003.
- [13] W. Kendall Melville, F. C. Felizardo, and Peter Matusov, "Wave slope and wave age effects in measurements of EM bias," See <http://airsea.sio.ucsd.edu>, in review.
- [14] C.P. Gommenginger, M.A. Srokosz, J. Wolf, and P.A.E.M. Janssen, "A theoretical investigation of altimeter sea state bias," *Journal of Geophysical Research*, vol. 108, no. C1, 2003.
- [15] T. Elfouhaily, D. R. Thompson, B. Chapron, and D. Vandemark, "Improved electromagnetic bias theory: Inclusion of hydrodynamic modulations," *Journal of Geophysical Research*, vol. 106, no. C3, pp. 4655–4664, March 15 2001.
- [16] W. Alpers and K. Hasselmann, "The two-frequency microwave technique for measuring ocean-wave spectra from an airplane or satellite," *Boundary Layer Meteorology*, vol. 13, pp. 215–230, 1978.
- [17] Karl F. Warnick, David V. Arnold, Floyd W. Millet, and W. Kendall Melville, "Theoretical model of EM bias based on RMS long-wave slope," *Journal of Geophysical Research*, 2004, in review.
- [18] Ernesto Rodriguez, Yunjin Kim, and Stephen L. Durden, "A numerical assessment of rough surface scattering theories: Horizontal polarization," *Radio Science*, vol. 27, no. 4, pp. 497–513, July-August 1992.
- [19] T. Elfouhaily, B. Chapron, and K. Katsaros, "A unified directional spectrum for long and short wind-driven waves," *Journal of Geophysical Research*, vol. 102, no. C7, pp. 15781–15796, July 15 1997.
- [20] Floyd W. Millet and Karl F. Warnick, "Validity of rough surface backscattering models," In press, 2004.
- [21] Karl F. Warnick, Floyd W. Millet, and David V. Arnold, "Physical and geometrical optics for 2D rough surfaces with power-law height spectra," *IEEE Transactions on Antennas and Propagation*, 2004, in review.
- [22] D. V. Arnold, W. K. Melville, R. H. Stewart, J. A. Kong, W. C. Keller, and E. Lamarre, "Measurements of electromagnetic bias at Ku and C bands," *Journal of Geophysical Research*, vol. 100, no. C1, pp. 969–980, January 15 1995.